Dc and Ac conductivity of $La_2CuO_{4+\delta}$

P. Lunkenheimer[1], G. Knebel[1], A. Pimenov[1], G.A. Emel'chenko[2], A. Loidl[1]

[1] Institut für Festkörperphysik, Technische Hochschule Darmstadt, D-64289 Darmstadt, Germany
[2] Institute of Solid State Physics, Russian Academy of Sciences, Chernogolovka, Russia

Abstract. The complex conductivity of $La_2CuO_{4+\delta}$ has been investigated for frequencies 20 Hz $\leq \nu \leq$ 4 GHz and temperatures 1.5 K $\leq T \leq$ 450 K. Two single crystals with $\delta \approx 0$ and $\delta \approx 0.02$ were investigated, using dc (four-probe), reflectometric and contact-free techniques. At high temperatures the dc conductivity is thermally activated with low values of the activation energy. For low temperatures Mott's variable range hopping dominates. The real and imaginary parts of the ac conductivity follow a power-law dependence $\sigma \sim \nu^s$, typical for charge transport by hopping processes. A careful analysis of the temperature dependence of the ac conductivity and of the frequency exponent s has been performed. It is not possible to explain all aspects of the ac conductivity in $La_2CuO_{4+\delta}$ by standart hopping models. However, the observed minimum in the temperature dependence of the frequency exponent s strongly suggests tunneling of large polarons as dominant transport process.

PACS: 72.20.Fr.; 72.80.Jc; 74.70.Vy

1. Introduction

Among the parent compounds of the high-temperature superconductors, $La_2CuO_{4+\delta}$ has found most attention due to its relative simple structure and the possibility to change its electronic and magnetic behavior in a wide range by the variation of the charge carrier density. This can be achieved either by doping with an acceptor metal like Ba or Sr, or by doping with excess oxygen, which can easily be introduced by annealing procedures. Although a large amount of experimental work on the electrical properties of this system has been performed, results on the ac response of La_2CuO_4 are still scarce and often at variance to each other. Evidence for extremely heavy charge carriers and a high dielectric constant has been reported from millimeter-wave conductivity measurements [1]. However, these results are at odds with results of ac conductivity measurements at audio and radio frequencies [2, 3]. In these experiments a frequency dependent ac conductivity characterized by a power law, $\sigma \sim \nu^s$ with $s < 1$, has been found, which gives evidence for hopping conductivity [4, 5]. Up to now the question of the predominant hopping mechanism in La_2CuO_4 is still unresolved. For $\delta \approx 0$ Chen et al. [2] have found a highly temperature dependent exponent s, which was the same for both crystallographic directions. Their investigation was restricted to temperatures $T < 12$ K where contributions of the electrical contacts can be neglected. By assuming a contribution of multiple hops these authors interpreted their results to be consistent with phonon-assisted tunneling of electrons between localized states [2]. Due to the higher measuring frequencies (up to 1 GHz) we were able to give information on the hopping properties at temperature $T > 25$ K [3]. We found an almost temperature independent and highly anisotropic exponent s which seemed at variance with the results of Chen et al. [2].

In order to clarify these discrepancies we carried out measurements of the ac conductivity of single crystals of $La_2CuO_{4+\delta}$ at temperatures 1.5 K $\leq T \leq$ 450 K. For the doped ($\delta \approx 0.02$) and undoped ($\delta \approx 0$) samples we found $\sigma' \sim \nu^s$. We compare our results to the predictions of various models on hopping conductivity. In addition, to ensure the intrinsic nature of the hopping conductivity we carried out contact-free measurements.

2. Experimental details

Single crystals of $La_2CuO_{4+\delta}$ were grown by slow cooling using a rotating crucible. For details on the sample preparation see [6]. In addition, to introduce excess oxygen, some single crystals have been annealed under continuous oxygen flow at $T = 600\,^\circ$C for 12 h. δ has been determined from the lattice constants at room temperature [7] and from the onset temperature of the phase separation process (see below).

Reflectometric and contact-free measurement techniques have been employed to determine the real part σ' and the imaginary part σ'' of the complex conductivity in

the radiofrequency range. For the reflectometric measurements the sample has been mounted at the end of a coaxial air line, connecting the inner and outer conductors [8]. The complex reflection coefficient Γ of this assembly has been recorded using an HP4191 impedance analyzer for frequencies 1 MHz $\leq \nu \leq$ 1 GHz and an HP8510 network analyzer for frequencies 100 MHz $\leq \nu \leq$ 4 GHz. The complex conductivity can be calculated from Γ after proper calibration using three standard samples to eliminate the influence of the coaxial line and the sample holder. For cooling, the end of the line with the sample holder has either been connected to the cold head of a closed cycle refrigerator [8] or brought into a ^{4}He cryostat.

Reflectometric methods require two-point contact configurations. Thus, to make electrical contacts the two surfaces of the crystal normal to the field direction have been covered with silver paint. Silver paint contacts have the advantage of being easily removable which allows the investigation of the same crystal in different crystallographic directions. However, such contacts have a large resistance at low frequencies, which has to be accounted for in the data analysis.

As the separation of contact and intrinsic contributions in the data analysis of the two-point measurements is a rather difficult task it would be very desirable to measure the pure sample response without contacts. For this purpose, a contact-free measuring method has been developed, which has been applied on the same single crystals. The idea of the measurement is to determine the resonance frequency ν_0 and the quality factor Q of an LC circuit at resonance conditions with and without sample. In this experimental set-up the sample is placed between two capacitor plates. The complex conductivity is then evaluated measuring the changes of the resonator properties caused by the sample. Details of this method are given elsewhere [9]. In addition, the dc conductivity has been investigated using standard four-probe techniques.

All measurements have been performed along the three crystallographic directions of the crystals. Hence, the field was oriented within the CuO_2 planes ($E \| a$ or $E \| b$) or perpendicular to them ($E \| c$). As a result of the twinning of the crystal it is not possible to distinguish the two in-plane directions. For convenience in the following the in-plane measurements are denoted as $E \| a$.

3. Results and discussion

3.1. DC measurements

The temperature dependence of the dc conductivity for the sample with $\delta \approx 0$ is presented in Fig. 1 for both field directions. Here we have plotted the data using two alternative representations, namely: i) $\log(\sigma)$ vs. $1/T$ and ii) $\log(\sigma)$ vs. $1/T^{1/4}$. Using these representations, straight lines indicate i) thermally activated behavior:

$$\sigma_{dc} \sim \exp(E_g/k_B T) \tag{1}$$

or ii) Mott variable range hopping (VRH) [10]:

$$\sigma_{dc} \sim \exp(T_0/T)^{1/4} \tag{2}$$

Here E_g is the activation energy which in a semiconductor would correspond to the half width of the bandgap. In the VRH model T_0 is proportional to $\alpha^3/N(E_F)$, with α the inverse of the localization length and $N(E_F)$ the density of states at the Fermi level [10].

At low temperatures, $T < 30$ K, the data are well described by Mott's $T^{1/4}$ law. At higher temperatures only nearest-neighbor-hops become significant [10] and the conductivity is simply thermally activated. The main parameters resulting from the fits in Fig. 1 are given in Table 1. They are in approximate agreement with literature data, which are also given in Table 1.

An activation energy of $E_g \approx 30$ meV as inferred from conductivity measurements seems rather small and is at variance with the optical gap energy $E \approx 2$ eV [14, 15]. La_2CuO_4 can be regarded as a charge transfer insulator with the two uppermost bands being the empty upper (Cu 3d) Hubbard band and a filled O 2p band. From infrared reflectivity measurements [16, 17] it is known that in lightly doped La_2CuO_4 a midinfrared absorption band appears at ~ 0.13 eV. The large difference between the optical (0.13 eV) and the thermal (0.03 eV) activation energy is believed to be due to polaronic impurity states [17]. Adopting Mott's picture for localization of charge carriers [10], the mobility edge can be assumed near the upper band edge of the O 2p band. At low temperatures

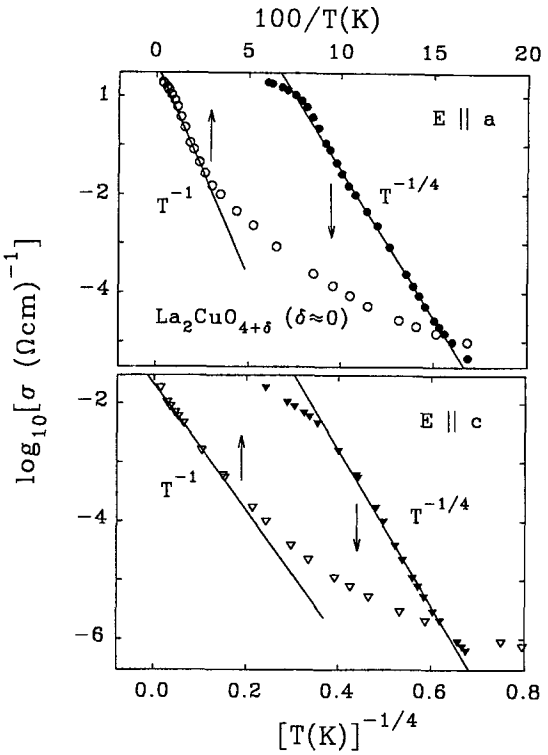

Fig. 1. Dc conductivity of $La_2CuO_{4+\delta}$ ($\delta \approx 0$) for the field oriented parallel (upper frame) and perpendicular (lower frame) to the CuO_2 planes. The same data are plotted vs. T^{-1} (open symbols) and vs. $T^{-1/4}$ (closed symbols). In certain temperature regions the curves approach straight lines which indicates thermally activated and VRH behavior respectively

Table 1. Various parameters characterizing the electrical properties of $La_2CuO_{4+\delta}$ ($\delta \approx 0$). T_0 and E_g are defined in (1) and (2), respectively. σ_{ab} and σ_c are the dc conductivities for $E \| a$ and $E \| c$

$T_0(E \| a)$ [K]	$T_0(E \| c)$ [K]	$E_g(E \| a)$ [meV]	$E_g(E \| c)$ [meV]	$\sigma_{ab}(300\ K)$ [$\Omega^{-1}cm^{-1}$]	$\sigma_c(300\ K)$ [$\Omega^{-1}cm^{-1}$]	ε_{∞} ($E \| a$)	ε_{∞} ($E \| c$)	Ref.
$1.5 \cdot 10^6$	$1.0 \cdot 10^6$	34	18	1.9	$1.8 \cdot 10^{-2}$	54	28	this work
$6.1 \cdot 10^5$				$3 \cdot 10^{-2}$	$2 \cdot 10^{-2}$		41	[3]
		42	27	4	$1 \cdot 10^{-2}$			[11]
$1.4 \cdot 10^5$				0.2				[12]
				5		45	23	[13]
						35	28	[2]

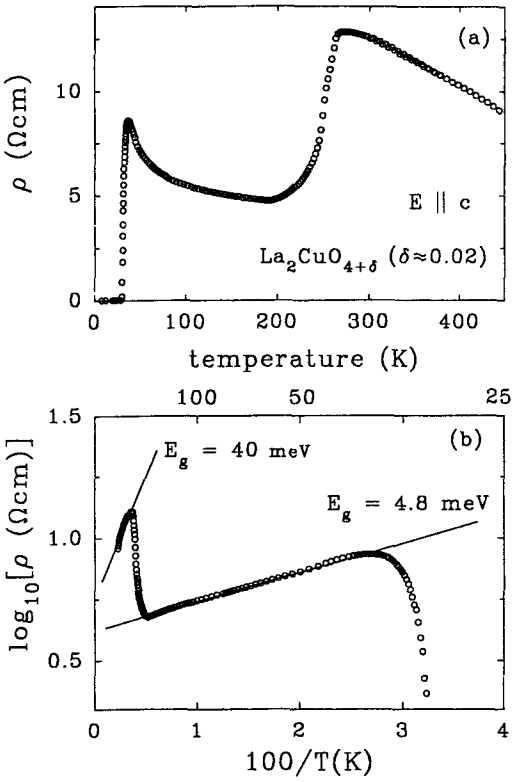

Fig. 2. Temperature dependence of the dc resistivity of oxygen annealed $La_2CuO_{4+\delta}$ ($\delta \approx 0.02$) in linear **a** and Arrhenius representation **b** for $E \| c$

only electrons within the localized states can be excited into the impurity level, hence showing hopping conductivity.

In addition, Table 1 contains the absolute value of the dc conductivity at room temperature. $\sigma_{dc}(300\ K)$ of our crystal agrees well with values from literature for both field directions. However, $\sigma_{dc}(300\ K)$ for $E \| a$ of the crystal examined earlier [3] is approximately two orders of magnitude lower than expected. For this finding we have no explanation.

Now we focus on the oxygen annealed crystal with $\delta \approx 0.02$. Figure 2a shows the temperature dependence of the dc resistivity of this crystal for $E \| c$. Two distinct features can be seen: *i*) The resistivity becomes zero at $T_c \approx 30$ K, i.e. the sample becomes superconducting (at least spurious amounts along a percolating path). *ii*) With lowering of the temperature the resistivity falls about a factor of 3 between 270 and 200 K. Such a step in $\rho(T)$ of oxygen annealed crystals has been found before [18, 19, 20] and can be ascribed to a phase separation occurring in $La_2CuO_{4+\delta}$ for $0.01 < \delta < 0.055$ [18, 21, 22], which is accompanied by the diffusion of oxygen ions. For $\delta \approx 0.02$ the sample should separate in two phases with $\delta \approx 0.055$ and $\delta \approx 0.01$ [22]. In the phase separated state the sample can be approximated by an equivalent circuit of two resistors in parallel, which account for the highly different resistivities of the oxygen-rich ad oxygen-poor phase. Therefore at $T < 200$ K mainly the oxygen-rich phase contributes to the observed resistivity. In Fig. 2b the same data are shown in an Arrhenius representation. It becomes obvious that the resistivity in the phase separated state follows a thermally activated behavior similar to the results on the crystal with $\delta \approx 0$ in this temperature range (Fig. 1). However, now the energy barrier is even lower, $E_g = 4.8$ meV. Such a low value has also been found by Bazhenov [23] in oxygen doped crystals. This indicates, that now the impurity states are almost at the upper bound of the O 2p band. Hence, this compound with $\delta \approx 0.02$ is very close to the insulator to metal transition. Above the phase separation temperature, the temperature dependence is much stronger but only roughly follows an Arrhenius behavior with $E_g \approx 40$ meV, a value which lies in the same range as for the unannealed crystal.

3.2. *Ac measurements*

3.2.1. Reflectometric method. Figure 3 shows the frequency dependence of the real part of the conductivity σ' and of the dielectric constant ε' for various temperatures with $E \| c$. ε' has been calculated from σ'' by $\varepsilon' = \sigma''/(\omega \varepsilon_0)$ with ε_0 the dielectric constant of the vacuum and $\omega = 2\pi\nu$. At low frequencies $\sigma'(\nu)$ exhibits a steplike increase while $\varepsilon'(\nu)$ shows a steplike decrease with increasing frequency. For lower temperatures, both phenomena shift to lower frequencies. This behavior completely is due to the electrical contacts which usually can be described by an equivalent circuit consisting of the contact resistance R_c (frequency independent but with a semiconducting temperature behavior) parallel to the contact capacitance C_c (frequency and temperature independent). The frequency and temperature dependent sample resistance R_s, in series with this leaky capacitor accounts for the results described above. The point of inflection of the $\sigma'(\nu)$ step is

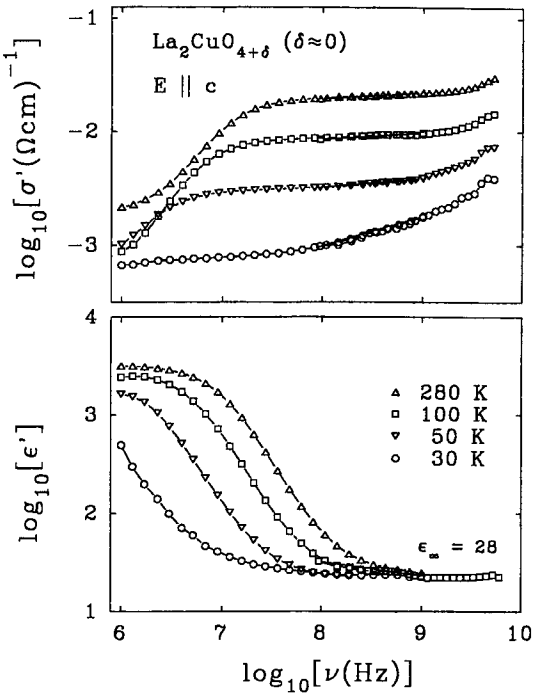

Fig. 3. Frequency dependence of the real parts of the conductivity (upper frame) and the dielectric constant (lower frame) of $La_2CuO_{4+\delta}$ ($\delta \approx 0$) for various temperatures with $E \| c$ (double logarithmic plot).

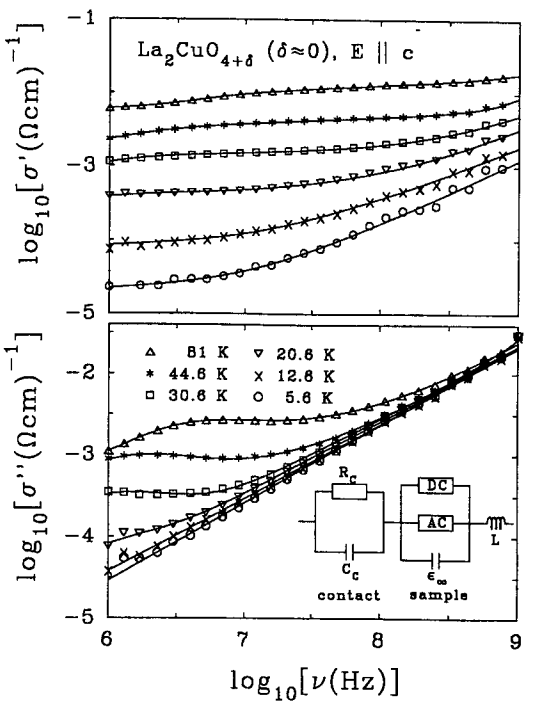

Fig. 4. Frequency dependence of real and imaginary part of the conductivity of $La_2CuO_{4+\delta}$ ($\delta \approx 0$) for various temperatures below 81 K with field direction $E \| c$. The lines are the results of fits using the equivalent circuit indicated. For the intrinsic sample conductivity the validity of the UDR has been assumed

located at

$$\nu_p = \frac{1}{2\pi C_c} \cdot \left[\frac{1}{R_c} + \frac{1}{R_s}\right] \tag{3}$$

which explains the observed shift of the contact phenomena as both R_s and R_c are expected to exhibit a semiconductor-like temperature dependence (compare also Fig. 1).

At frequencies higher than the steplike increase of $\sigma'(\nu)$ and higher than the steplike decrease of $\varepsilon'(\nu)$, the intrinsic sample conductivity is measured with the contact resistance being shortened by C_c. At frequencies directly above the step, $\sigma'(\nu)$ shows a plateau which can be identified with the dc conductivity σ_{dc}. At higher frequencies $\sigma'(\nu)$ increases continuously. This is typical for hopping conduction processes [4, 5, 24]. At high frequencies $\varepsilon'(\nu)$ is dominated by the high frequency dielectric constant ε_∞ of the crystal to which the electronic and ionic polarizability contribute. ε_∞ can easily be read off in Fig. 3 to be $\varepsilon_\infty = 28$ (± 2). This is in agreement with the results of Reagor et al. [1] and Chen et al. [2] (see Table 1).

In order to study the hopping conductivity of $La_2CuO_{4+\delta}$ in more detail, investigations at lower temperatures are necessary. Results obtained at temperatures $5.6 \leq T \leq 81$ K are shown in Fig. 4. The step in $\sigma'(\nu)$ and the maximum in $\sigma''(\nu)$ are caused by the contacts as discussed above. For the lowest temperatures and in the frequency window investigated the intrinsic sample response is dominant. Therefore the measurements on $La_2CuO_{4+\delta}$ single crystals reported in Ref. [2] have been restricted to low temperatures. The frequency dependence of the intrinsic sample conductivity can well be described by the so called universal dielectric response (UDR) [24]:

$$\sigma' = \sigma_{dc} + \sigma_0 \omega^s \tag{4}$$

There is a vast number of theoretical approaches to deduce this behavior from the microscopic transport properties of various classes of materials. Processes involving hopping over, or tunneling through an energy barrier separating different localized states have been considered for various kinds of charge carriers [4, 5, 24]. However, common to all theories is the result that $\sigma' \sim \nu^s$, which holds true at least in a limited frequency range. However, the UDR assumes an *exact* ν^s behavior (with frequency independent s) as it has been found experimentally for most hopping systems. Within this model σ'' can be written as:

$$\sigma'' = \sigma_0 \omega^s \tan(s\pi/2) + \varepsilon_0 \varepsilon_\infty \omega \tag{5}$$

The first term follows from the Kramers-Kronig transformation of (4) [25]. The second term takes the high frequency dielectric constant into account and leads to a slope of one for high frequencies in the double logarithmic plot (Fig. 4).

In order to describe the frequency dependence of σ' and σ'' at higher temperatures, the equivalent circuit indicated in Fig. 4 has been used. As mentioned above, the contacts are accounted for by a leaky capacitor in series to the sample. For the sample the UDR has been assumed

including σ_{dc} (described by a frequency independent resistor) and ε_∞ (a capacitor in parallel). In addition, all inductive contributions which may arise from the sample itself, from the contacts, or from the sample holder are described by an inductance placed in series. This equivalent circuit is the same as that used in our previous report [3] with the addition of ε_∞, ε_∞ becomes increasingly important at low temperatures and therefore cannot be omitted in the present analysis.

The results of fits using this circuit which have been carried out simultaneously on $\sigma'(\nu)$ and $\sigma''(\nu)$ are shown as solid lines in Fig. 4. Data and fit agree almost perfectly. The model involves seven parameters which e.g. for 30 K have values of $\sigma_{dc} = 1.48$ $(\mathrm{m\Omega cm})^{-1}$, $\sigma_0 = 7.4 \cdot 10^{-11}$ $(\Omega\mathrm{cm})^{-1} s^{0.77}$, $s = 0.77$, $R_c = 2.7\ \mathrm{k\Omega}$, $\varepsilon_\infty = 24$, $C_c = 90$ pF, and $L = 3$ nH. The values of σ_{dc}, extracted from the fits are in agreement with the four-point data of Fig. 1.

Important information concerning the microscopic hopping process can be gained from the absolute value and the temperature dependence of the frequency exponent s. Coming from low temperatures, s decreases significantly and shows a minimum at about 50 K. This is at variance with the results obtained by us on a single crystal from a different source being reported in [3]. In [3] fits using the equivalent circuit of Fig. 4 yielded an $s(T)$ which was very small ($s \approx 0.2$) and almost temperature independent down to the lowest temperature available to us at that time ($T \approx 25$ K). However, the fits in Fig. 4 of [3] show large deviations at low frequencies as already mentioned there. We now have solved these problems by taking into account a distribution for the leaky capacitor representing the contacts. For the frequency dependent impedance of the leaky capacitor, $Z = R_c/(1 + (\mathrm{i}\omega\tau)^{1-\alpha})$ has been assumed with $0 < \alpha < 1$ and $\tau = R_c C_c$. The exponent $\alpha > 0$ leads to a broadening of the contact step in $\sigma'(\nu)$ and of the corresponding maximum in $\sigma''(\nu)$ which can be regarded as arising from a distribution of relaxation times τ, called Cole-Cole distribution [26]. The case $\alpha = 0$ corresponds to a single relaxation time. Fits using this distribution are shown as solid lines together with the data from [3] in Fig. 5. Now the agreement of fit and data is very good yielding an $s(T)$ which decreases with decreasing T.

The frequency exponents s as function of temperature as deduced from these experiments are shown in Fig. 6. To check the error of s, we fixed s at various values above and below the result of the "free" fit until the deviations between data and fit were significantly larger than the error of the data. This procedure reveals large error bars of s at temperatures $T > 20$ K which is due to the dominance of σ_{dc} and the contact contributions at high temperatures. Within these error bars the results from both measurements match together well thereby corroborating the significance of the minimum in $s(T)$.

Now we turn to our results with the field directed parallel to the CuO_2 planes. Figure 7 shows the frequency dependence of σ' and σ'' for various temperatures $T \leq 79$ K. Due to the higher dc conductivity for $E \| a$ (see Fig. 1) the contact steps are now shifted to higher frequencies. A purely intrinsic response is only observed for temperatures $T \leq 10$ K. The maximum observed in $\sigma'(\nu)$ at 79 K is due to the inductive contributions mentioned above and is, at the highest frequencies investigated, accompanied by negative values of σ''. The solid lines included in Fig. 7 are the results of fits using the same equivalent circuit as for $E \| c$ but with the inclusion of a Cole-Cole distribution for the contact relaxation time. Again very good fits have been obtained. The parameters

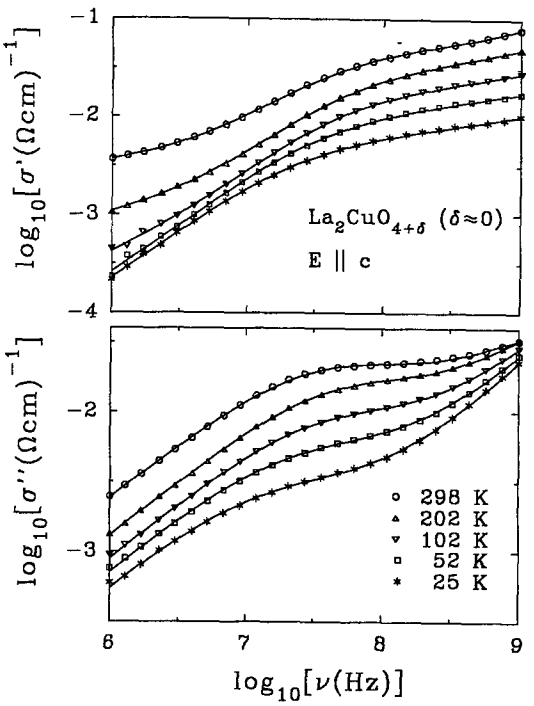

Fig. 5. Frequency dependence of real and imaginary part of the conductivity of a $La_2CuO_{4+\delta}$ ($\delta \approx 0$) single crystal from a different crystal grower as already published in [3]. The results are shown for various temperatures with field direction $E \| c$. The solid lines are fits using the equivalent circuit indicated in Fig. 4. In contrast to Ref. [3] for the relaxation time of the leaky capacitor which describes the contacts a Cole–Cole distribution has been assumed

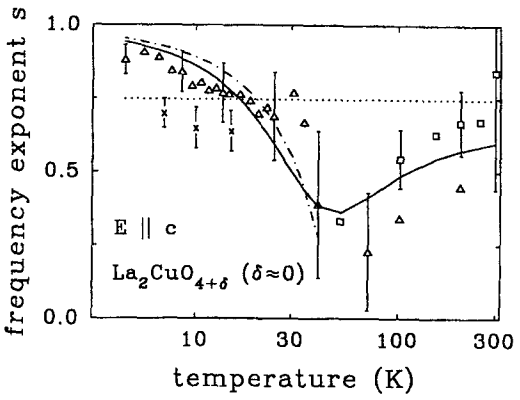

Fig. 6. Temperature dependence of the frequency exponent s determined from fits as described in the text. Shown are results from reflectometric measurements on two different single crystals (□, △) and from contact free measurements (×). The lines have been calculated using various models for hopping conductivity, namely: dotted - QMT, solid - OLPT, dash-dotted-CBH

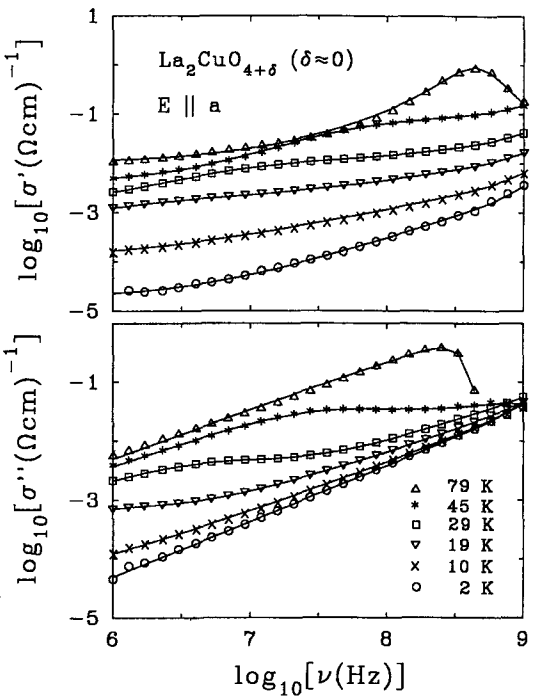

Fig. 7. Frequency dependence of σ' and σ'' of $La_2CuO_{4+\delta}$ ($\delta \approx 0$) for various temperatures $T \leq 79$ K with field direction $E \| a$. The lines are the results of fits using the equivalent indicated in Fig. 4 with the inclusion of a Cole–Cole distribution for the contact relaxation time

for $T = 29$ K are: $\sigma_{dc} = 12.8\ (\mathrm{m\Omega cm})^{-1}$, $\sigma_0 = 1.5 \cdot 10^{-9}$ $(\Omega\mathrm{cm})^{-1}\mathrm{s}^{0.74}$, $s = 0.74$, $R_c = 1.8\ \mathrm{k\Omega}$, $C_c = 230$ pF, $L = 1.0$ nH, $\alpha = 0.21$. $\sigma_{dc}(T)$ is in accord with the dc results presented in Fig. 1. The exponent $s(T)$ is shown in Fig. 8 (triangles). Again s decreases significantly with T at low temperatures and exhibits a minimum at about 20 K. The s values at three low temperatures reported by Chen et. al. [2] which are also shown in Fig. 8 (diamonds) match well with our data. It is interesting to note that the measurements of Chen et al. have been carried out at frequencies 1 kHz $\leq \nu \leq$ 10 MHz while our results have been obtained at 10 MHz $\leq \nu \leq$ 1 GHz. This fact implies that s is frequency independent over 6 decades of frequency (i.e. it follows the UDR prediction). Such a behavior is at variance with the predictions of most theories on hopping conductivity [4, 5], but has nevertheless been found in many materials [24].

In addition, in Fig. 8 we included the results on the single crystal from a different crystal grower with $E \| a$ which already have been reported [3] (squares). Here it was possible to determine $s(T)$ successfully up to room temperature, which was due to the contact step occurring at much lower frequencies than in the more recent measurements. The latter is mainly due to the untypical high dc resistance of this sample (compare Eq. (3)).

Now we turn to our results on the ac conductivity of the oxygen annealed crystal ($\delta \approx 0.02$). Figure 9 shows the frequency dependence of the real and imaginary part of the conductivity for $E \| c$. Contact effects dominate in most of the frequency range, which is due to the lower resistance of this sample (compare Eq. (3)). Before $\rho(T)$

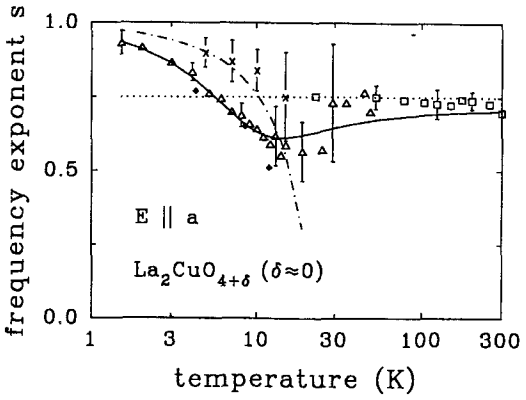

Fig. 8. Temperature dependence of the frequency exponent s as resulting from fits as described in the text. Shown are results from reflectometric measurements on two different single crystals (△, □) and results obtained using a contact free measuring technique (×). In addition, the s-values reported by Chen et al. [2] are included (◆). The lines have been calculated using various hopping models, namely: dotted line – QMT, solid line – OLPT, dash-dotted line – CBH

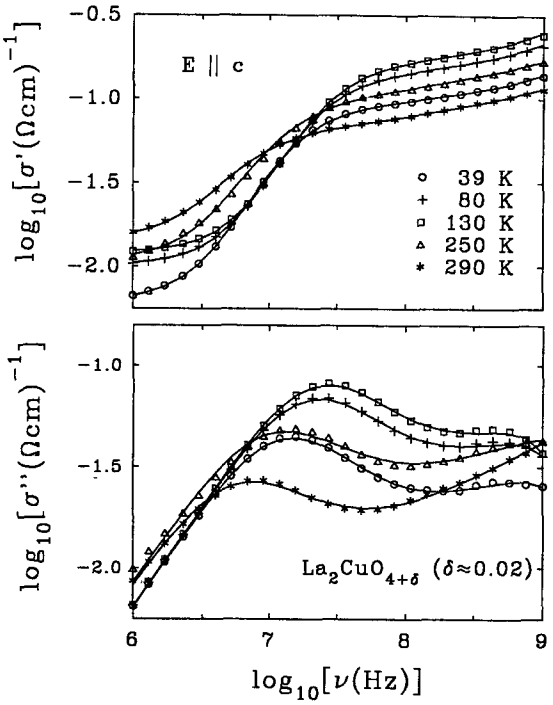

Fig. 9. Frequency dependence of σ' and σ'' of $La_2CuO_{4+\delta}$ ($\delta \approx 0.02$) for various temperature with $E \| c$. The solid lines are the results of fits using the equivalent circuit indicated in Fig. 4 with a Cole–Cole distribution for the contact relaxation time

rises high enough to shift the contact effects out of the frequency window the sample becomes superconducting. The solid lines in Fig. 9 are the results of fits using the same equivalent circuit as described above. Data and fit agree very well but, however, the resulting s of approximately $s \approx 0.5$ has large error bars of $\Delta s \approx 0.3$. Therefore no statement on the temperature dependence of s can be made. However, the data can only be satisfactorily described assuming hopping conductivity for the intrinsic

response of the sample. This is correct either for temperatures above or below the phase separation. This finding implies that also in the more metallic phase with $\delta \approx 0.05$, which dominates the conductivity in the phase separated state [22], localization of charge carriers is important.

3.2.2. Contact-free measurements. Contact-free measurements have been performed for the crystal with $\delta \approx 0$ at three measuring frequencies. The results are shown in Fig. 10, together with the dc data from Fig. 1. At high temperatures, $T > 40$ K, for both field directions the measured $\sigma'(T)$ closely follows the dc behavior. At lower temperatures σ' deviates from the dc curve thereby exhibiting a clear increase with frequency. The frequency dependence of σ' can well be fitted using eq. (4). The fits yield an $s(T)$ (crosses in Figs. 6 and 8) which is in fair agreement with $s(T)$ from the reflectometric measurements. Of course, it is quite difficult to extract quantitative information on $s(T)$ from three frequency-points only. Hence, the error bars are large. However, having in mind that up to now all experiments performed on the ac conductivity of La_2CuO_4 measured the response of the sample *and* the contacts our results are a convincing confirmation of the intrinsic nature of the power-law behavior, $\sigma \sim \nu^s$. They also corroborate the validity of the evaluation procedure which we applied on the "contact-data".

3.2.3. Discussion of the ac results. In the following we will compare our results on $s(T)$ and $\sigma_{ac}(T)$ to the predictions of various models for hopping conductivity.

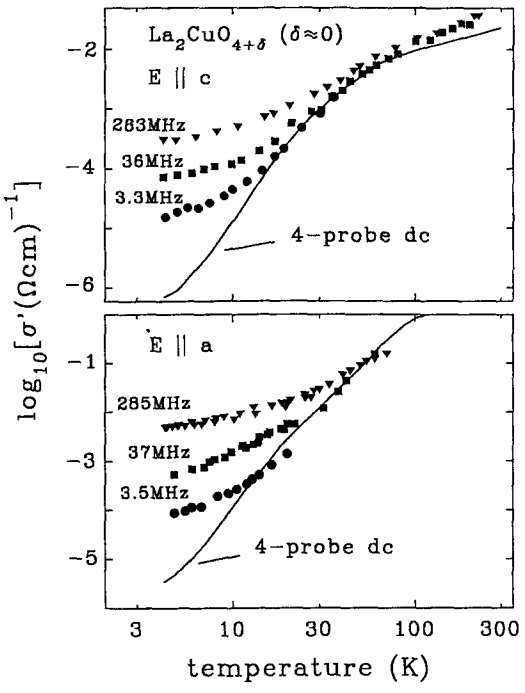

Fig. 10. Temperature dependence of the conductivity of $La_2CuO_{4+\delta}$ ($\delta \approx 0$) for three frequencies with field directions $E \| c$ (upper frame) and $E \| a$ (lower frame). The data have been obtained using a contact free measuring technique. Also shown are dc results from conventional four point measurements

Taking together all data collected on $La_2CuO_{4+\delta}$ with $\delta \approx 0$ (Figs. 6 and 8) a quite clear picture for the temperature dependence of $s(T)$ arises: $s(T)$ exhibits a minimum at $T \approx 50$ K for $E \| c$ and at $T \approx 20$ K for $E \| a$ which at least for $E \| c$ can be regarded as significant. For $T \to 0$ K the exponent increases strongly, which for $E \| a$ has already be seen in the low temperature measurements of Chen et al. [2] (closed diamonds in Fig. 8). In regard of the temperature dependence of the dc conductivity these authors interpreted their data as being characteristic for quantum-mechanical tunneling (QMT) of holes. However, as this model predicts a temperature independent exponent s (indicated as dotted line in Figs. 6 and 8) [4, 5], multiple hopping [27] had to be assumed to explain the observed strong temperature dependence, at least qualitatively. Multiple hopping is predicted to occur at high temperatures and low frequencies and leads to a lowering of the frequency exponent s [27]. For higher frequencies hopping should occur between two neighbouring sites only and therefore s should increase. However, experimentally s seems to be constant from 1 kHz to 1 GHz and hence it is unlikely that multiple hops play an important role in La_2CuO_4. In addition, $s(T)$ does not approach a limiting value of 0.8 for $T \to 0$ K as assumed by Chen et al. but increases further up to values of 0.9 for the lowest temperatures investigated by us (Figs. 6 and 8). Even then no saturation can be seen, but s seems to approach a limiting value of 1 for $T \to 0$ K. Such high values of s can hardly be obtained in the QMT model [28] which clearly shows that QMT is not the dominant conduction process in La_2CuO_4 at low temperatures.

Alternative explanations for the observed hopping conductivity including the approach of a value of 1 for $T \to 0$ K are given by the "Overlapping Large Polaron Tunneling" (OLPT) model and by the "Correlated Barrier Hopping" (CBH) model [4, 5].

In the OLPT model [4, 5, 29] the charge carriers are assumed to be large polarons. "Large" means that the lattice distortion around a site of a charge extends over several atomic distances which causes an overlap with the distortions on neighboring sites. This gives rise to an energy barrier which is a function of the site separation. In the OLPT model the frequency dependence of the conductivity can be expressed by $\sigma \sim \nu^s$. The temperature dependence of s is given by [4]:

$$s = 1 - \frac{8\alpha R_W + 6\beta W_{HO}(r_0/R_W)}{[2\alpha R_W + \beta W_{HO}(r_0/R_W)]^2} \tag{6}$$

with $\beta = 1/(k_B T)$. W_{HO} is the barrier height for infinite site separation, r_0 is the polaron radius, α is the spatial extent of the localized state wavefunction and R_W is the hopping distance, given by

$$R_W = \frac{1}{4\alpha}\{[\ln(1/\omega\tau_0) - \beta W_{HO}] + ([\ln(1/\omega\tau_0) - \beta W_{HO}]^2 + 8\alpha r_0 \beta W_{HO})^{1/2}\} \tag{7}$$

τ_0 is the characteristic relaxation time, which should be of the order of a typical phonon frequency. The solid lines in Figs. 6 and 8 have been calculated using (6) and (7). The main parameters were: $W_{HO} = 45$ meV, $\tau_0 = 10^{-12}$ s,

$\alpha r_0 = 0.68$ for $E \| c$ and $W_{HO} = 12$ meV, $\tau_0 = 10^{-14}$s, $\alpha r_0 = 1.6$ for $E \| a$. It should be noted that for high temperatures, s as deduced from the OLPT model, approaches the constant value as predicted by the QMT model. This behavior is documented in Fig. 8. Obviously the OLPT model can explain the temperature dependence of the frequency exponent s in La_2CuO_4 within the error bars. We want to emphasize that, to our knowledge, the OLPT model is the only model that predicts a minimum in the temperature dependence of the frequency exponent which strongly suggests polarons as charge carriers in La_2CuO_4. Note that W_{HO} lies in the same order of magnitude as the gap energy deduced from the temperature dependence of the dc conductivity (see Table 1). The difference of W_{HO} for $E \| a$ and $E \| b$ which leads to a different position of the minimum of $s(T)$ (it is located at approximately $0.1 \cdot W_{HO}/k_B$ [4]) is in accord with the observed anisotropy of the absolute value of the conductivity. Both, the smaller values of W_{HO} and of τ_0 should lead to a higher conductivity for $E \| a$ as observed experimentally. The larger αr_0 for $E \| a$, which leads to a less pronounced minimum for this direction [4] points to a large polaron radius. This can be understood having in mind the higher ε_∞ for $E \| a$ (see Table 1) which implies a higher polarizability of the lattice in this direction.

The polaron coupling constant is proportional to $1/\varepsilon_e - 1/\varepsilon_\infty$ [30]. Here ε_e is the electronic contribution to the dielectric constant ($\varepsilon_e \approx 5$ [31], for ε_∞, see Table 1). This difference is rather high in La_2CuO_4 and the occurrence of polarons as charge carriers seems reasonable [2]. Evidence for polarons in La_2CuO_4 has also been reported by Falck et al. [15] from the temperature dependence of the charge-transfer spectrum. In addition, experimental evidence for polaron hopping has been reported in a large number of superconducting cuprates [32] and in semiconducting $Bi_4Sr_4Ca_3Cu_4O_x$ [33] and $PrBa_2Cu_3O_{7-\delta}$ [34]. In this context it is interesting to note that there are speculations that the superconductivity in the cuprates could be due to the condensation of bipolarons [35, 36, 37].

The OLPT model also makes predictions on the temperature dependence of the ac conductivity σ_{ac}:

$$\sigma_{ac} = \frac{\pi^4}{12} \frac{N(E_F)^2 (k_B T)^2 e^2 \omega R_W^4}{2\alpha k_B T + W_{HO} r_0 / R_W^2}. \tag{8}$$

Here $N(E_F)$ is the density of states at the Fermi level. Figures 11 and 12 show the temperature dependence of σ_{ac} at three frequencies for $E \| c$ and $E \| a$, respectively. σ_{ac} has been calculated by subtracting σ_{dc} from the measured $\sigma(T)$. σ_{dc} has been taken from the fits of $\sigma(\nu)$ (see paragraph 3.2.1). In Figs. 11 and 12 the temperature range has been restricted to $T < 25$ K. At these low temperatures contact contributions can be neglected (compare Figs. 4 and 7). The solid lines in Figs. 11 and 12 are the results of fits using equations (6) and (7). Considering that additional errors may be introduced due to the subtraction of σ_{dc}, which occur especially at low frequencies, the fits are acceptable for $E \| c$. However, if all parameters are allowed to vary, W_{HO} tends to zero yielding simple (non-polaron) QMT. However, as mentioned above, neither the minimum in $s(T)$ nor the high s values exceeding 0.8 at low

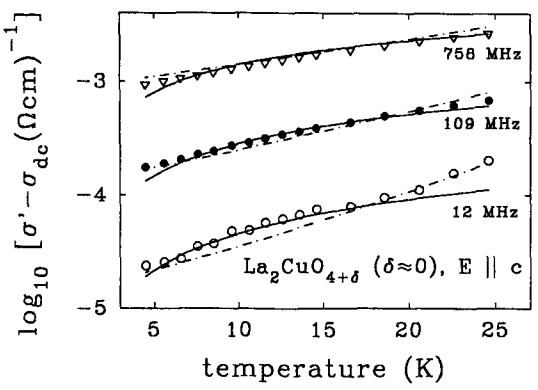

Fig. 11. Temperature dependence of the ac conductivity of $La_2CuO_{4+\delta}$ ($\delta \approx 0$) with $E \| c$ for various frequencies. The lines have been calculated using the OLPT model (solid lines) and the CBH model (dash-dotted lines)

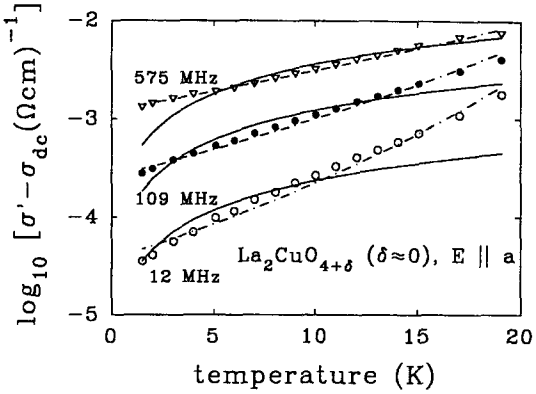

Fig. 12. Temperature dependence of the ac conductivity of $La_2CuO_{4+\delta}$ ($\delta \approx 0$) with $E \| a$ for various frequencies. The lines have been calculated using the OLPT model (solid lines) and the CBH model (dash-dotted lines)

temperatures can be explained by the QMT. Therefore we carried out fits with W_{HO} fixed at non-zero values. The highest value that still leads to acceptable fits (shown in Fig. 11) is $W_{HO} = 9$ meV. However, such a low W_{HO} does not lead to a satisfactory description of the minimum in $s(T)$ (Fig. 6). For $E \| a$ the situation is even worse. The fits to the experimental data at 12 Mhz and 109 MHz, shown as solid line in Fig. 12, clearly deviate, especially at high temperatures. In addition, the resulting W_{HO} again is almost zero ($W_{HO} = 7$ μeV). Hence, the OLPT model does not satisfactorily describe the temperature dependence of σ_{ac} for $E \| a$. The above evaluation of the data has also been carried out using the modified OLPT model, which takes into account intersite correlation effects [4]. However, no better description of the data could be achieved.

We now turn to the CBH model, which was introduced by Pike [38] to account for the dielectric loss in scandium oxide films and later has been applied by Elliott [28] to explain the ac loss in chalcogenide glasses. In this model thermally activated hopping of the charge carriers over the energy barrier separating two localized sites is assumed. The energy barrier is of simple coulombic type

and reduced due to overlapping coulomb potentials as a function of site distance (i.e. the barrier height is "correlated" to the distance). In the single electron CBH model the temperature dependence of the ac conductivity is given by:

$$\sigma_{ac} = \pi^3/24 N^2 \varepsilon\varepsilon_0 \omega R_W^6 \tag{9}$$

The hopping distance R_W is:

$$R_W = \frac{e^2}{\pi\varepsilon\varepsilon_0 [W_m - k_B T \ln(1/\omega\tau_0)]}. \tag{10}$$

W_m is the barrier height for infinite intersite separation and thus corresponds to the energy to take the charge carrier from the defect state to the continuum. The results of fits using equations (9) and (10) are shown as dash-dotted lines in Figs. 11 and 12. The agreement of data and fit is clearly better than for the OLPT model. The resulting parameters are: $W_m = 53$ meV, $\tau = 1.9 \cdot 10^{-12}$ s for $E \| c$ and $W_m = 29$ meV, $\tau = 1.8 \cdot 10^{-12}$s for $E \| a$. Note that W_m lies in the range of the gap energy deduced from $\sigma_{dc}(T)$ (Table 1).

If the frequency dependence of the conductivity is parameterized as $\sigma \sim \nu^s$ the result of the CBH model for $s(T, \nu)$ is:

$$s = 1 - \frac{6 k_B T}{W_m - k_B T \ln(1/\omega\tau_0)}. \tag{11}$$

A decrease of s from unity with increasing temperature is predicted by this model. However, eq. (11) cannot produce a minimum in $s(T)$ restricting the application of the CBH model in $La_2CuO_{4+\delta}$ to temperatures $T < 40$ K for $E \| c$ and $T < 20$ K for $E \| a$. In Figs. 6 and 8 the dash-dotted lines have been calculated using the CBH model with the parameters obtained from the fits to $\sigma_{ac}(T)$ (see above). An acceptable agreement of the theoretical calculations with the experimental results at low temperatures can be stated at least for $E \| c$. However, for higher temperatures the model becomes pathological predicting negative s values. The reason for this behavior lies in the rather low value of W_m which is necessary to take account of the steep decrease of s at low temperatures.

4. Conclusions

The dc and the complex ac conductivity of $La_2CuO_{4+\delta}$ single crystals with $\delta \approx 0$ and $\delta \approx 0.02$ have been investigated at temperatures $1.5\ \mathrm{K} \leq T \leq 450\ \mathrm{K}$. For both oxygen contents we find hopping conductivity as the dominant charge transport process which leads to a conductivity $\sigma \sim \nu^s$. For the first time information about the temperature dependence of the frequency exponent s in a broad temperature range could be obtained. In addition we carried out contact-free measurements which corroborate the intrinsic nature of the hopping conductivity in $La_2CuO_{4+\delta}$. We find for $\delta \approx 0$ and for both field directions an exponent s that reaches a value of 0.9 for low temperatures, which excludes simple QMT as dominant hopping mechanism. At higher temperatures $s(T)$ exhibits a distinct minimum for both field directions. To our knowledge, such a minimum can only be explained assuming tunneling of large polarons as dominant charge transport process [4, 5]. The formation of polarons in $La_2CuO_{4+\delta}$ seems reasonable if one has in mind the rather big difference between ε_∞ and ε_e leading to a high polaron coupling constant. In addition, evidence for polarons in $La_2CuO_{4+\delta}$ has also been found by Falck et al. [15]. However, the temperature dependence of the ac conductivity, the discrepancy between dc (VRH) and ac results (no QMT), and the finding of a frequency independent exponent s over 6 decades of frequency are still unresolved and cannot be accounted for by standard hopping models.

This research was supported by the Sonderforschungsbereich 252 (Darmstadt/Frankfurt/Mainz/Stuttgart).

References

1. Reagor, D., Ahrens, E., Cheong, S-W., Migliori, A., Fisk, Z.: Phys. Rev. Lett. **62**, 2048 (1989)
2. Chen, C.Y., Preyer, N.W., Picone, P.J., Kastner, M.A., Jenssen, H.P., Gabbe, D.R., Cassanho, A., Birgeneau, R.J.: Phys. Rev. Lett. **63**, 2307 (1989); Chen, C.Y., Birgeneau, R.J., Kastner, M.A., Preyer, N.W., Thio, T.: Phys. Rev. B **43**, 392 (1991)
3. Lunkenheimer, P., Resch, M., Loidl, A., Hidaka, Y.: Phys. Rev. Lett. **69**, 498 (1992)
4. Long, A.R.: Adv. Phys. **31**, 553 (1982)
5. Elliott, S.R.: Adv. Phys. **36**, 135 (1987)
6. Emel'chenko, G.A., Massalov, V.M., Abrosimov, N.V., Koncnovich, P.A., Merzhanov, V.A., Tatarchenko, V.A., Shchegolev, I.F., Parsamyan, T.K.: Inorg. Mater. **26**, 1339 (1990)
7. Grenier, J.-C., Lagueyte, N., Wattiaux, A., Doumerc, J.-P., Dordor, P., Etourneau, J., Pouchard, M., Goodenough, J.B., Zhou, J.S.: Physica C **202**, 209 (1992); Radaelli, P.G., Jorgensen, J.D., Schultz, A.J., Hunter, B.A., Chou, F.C., Johnston, D.C.: Phys. Rev. B **49**, 6239 (1994)
8. Böhmer, R., Maglione, M., Lunkenheimer, P., Loidl, A.: J. Appl. Phys. **65**, 901 (1989)
9. Pimenov, A., Loidl, A.: Phys. Rev. B **50**, 4204 (1994)
10. Mott, N.F.: Philos. Mag. **19**, 835 (1969); Mott, N.F., Davis, E.A.: Electronic Processes in Non-Crystalline Materials. Oxford: Oxford University Press 1979
11. Preyer, N.W., Birgeneau, R.J., Chen, C.Y., Gabbe, D.R., Jenssen, H.P., Kastner, M.A., Picone, P.J., Thio, T.: Phys. Rev. B **39**, 11563 (1989)
12. Kastner, M.A., Birgeneau, R.J., Chen, C.Y., Chiang, Y.M., Gabbe, D.R., Jenssen, H.P., Junk, T., Peters, C.J., Picone, P.J., Thio, T., Thurston, T.R., Tuller, H.L.: Phys. Rev. B **37**, 111 (1988)
13. Reagor, D., Migliori, A., Cheong, S.W., Fisk, Z: Physica B **163**, 264 (1990)
14. Orenstein, J., Thomas, G.A., Rapkine, D.H., Bethea, C.G., Levine, B.F., Cava, R.J., Cooper, A.S., Johnson, D.W., Remeika, J.P., Rietman, E.A.: Novel Superconductivity. Wolf, S.A, Kreslin, V.Z. (eds.) New York: Plenum Press 1987
15. Falck, J.P., Levy, A., Kastner, M.A., Birgeneau, R.J.: Phys. Rev. Lett. **69**, 1109 (1992)
16. Thomas, G.A., Rapkine, D.H., Cooper, S.L., Cheong, S.W., Cooper, A.S., Schneemeyer, L.F., Waszczak, J.V.: Phys. Rev. B **45**, 2474 (1992)
17. Falck, J.P., Levy, A., Kastner, M.A., Birgeneau, R.J.: Phys. Rev. B **48**, 4043 (1993)
18. Hundley, M.F., Thompson, J.D., Cheong, S-W., Fisk, Z., Schirber, J.E.: Phys. Rev. B **41**, 4062 (1990)
19. Sigmund, E., Hizhnyakov, V., Kremer, R.K., Simon, A.: Z. Phys. B **94**, 17 (1994)

20. Itoh, M., Oguni, M., Kyomen, T., Tamura, H., Yu, J.D., Yanagida, Y., Inaguma, Y., Nakamura, T.: Solid State Commun. **90**, 787 (1994)
21. Jorgensen, J.D., Dabrowski, B., Pei, S., Hinks, D.G., Soderholm, L., Morosin, B., Schirber, J.E., Venturini, E.L., Ginley, D.S.: Phys. Rev. B **38**, 11337 (1988)
22. Radaelli, P.G., Jorgensen, J.D., Kleb, R., Hunter, B.A., Chou, F.C., Johnston, D.C.: Phys. Rev. B **49**, 6239 (1994)
23. Bazhenov, A.V., Gorbunov, A.V., Timofeev, V.B.: JETP **77**, 500 (1993)
24. Jonscher, A.K.: Dielectric Relaxation in Solids. London: Chelsea Dielectrics Press 1983
25. See e.g., Bode, H.W.: Network Analysis and Feedback Amplifier Design. Princeton: Van Nostrand 1945
26. Cole, K.S., Cole, R.H.: J. Chem. Phys. **9**, 341 (1941)
27. Pollak, M.: Phys. Rev. **138**, A1822 (1965)
28. Elliott, S.R.: Phillos. Mag. **36**, 1291 (1977)
29. Long, A.R., Balkan, N., Hogg, W.R., Ferrier, R.P.: Phillos. Mag. B **45**, 497 (1982)
30. Fröhlich, H.: Adv. Phys. **3**, 325 (1954)
31. Collins, R.T., Schlesinger, Z., Chandrashekhar, G.V., Shafer, M.W.: Phys. Rev. B **39**, 2251 (1989)
32. Mihailovic, D., Foster, C.M., Voss, K., Heeger, A.J.: Phys. Rev. B **42**, 7989 (1990)
33. Gosh, A., Chakravorty, D.: J. Phys. Condens. Matter **2**, 649 (1990)
34. Varyukin, S.V., Parfenov, O.E.: JETP Lett. **58**, 830 (1993)
35. Prelovsek, P., Rice, T.M., Zhang, F.C.: J. Phys. **C20**, L229 (1987)
36. Emin, D.: Phys. Rev. B **45**, 5525 (1992)
37. de Jongh, L.J.: Physica C **152**, 171 (1988)
38. Pike, G.E.: Phys. Rev. B **6**, 1572 (1972)